Quantum state transfer between two photons with polarization and orbital angular momentum via quantum teleportation technology

Shihao Ru,[1] Min An,[1] Yu Yang,[1] Rui Qu,[1] Feiran Wang,[1,2] Yunlong Wang,[1,*] Pei Zhang,[1] and Fuli Li[1]

[1]*Shaanxi Key Laboratory of Quantum Information and Quantum Optoelectronic Devices, School of Physics of Xi'an Jiaotong University, Xi'an 710049, China*

[2]*School of Science of Xi'an Polytechnic University, Xi'an 710048, China*

(Received 3 February 2021; accepted 21 April 2021; published 5 May 2021)

Quantum teleportation is a useful quantum information technology to transmit quantum states between different degrees of freedom. Here we report a quantum state transfer experiment in the linear optical system, transferring a single-photon state in the polarization degree of freedom (DoF) to another photon in the orbital angular momentum (OAM) quantum state via a biphoton OAM entangled channel. Our experimental method is based on quantum teleportation technology. The differences between ours and the original teleportation scheme is that the transfer state is known in ours, and our method is for different particles with different DoFs, while the original one is for different particles with the same DoF. In addition, our present experiment is implemented with a high Bell efficiency since each of the four hybrid-entangled Bell states can be discriminated. We use six states of poles of the Bloch sphere to test our experiment, and the fidelity of the quantum state transfer is $91.8 \pm 1.3\%$.

DOI: 10.1103/PhysRevA.103.052404

I. INTRODUCTION

Quantum entanglement is one of the most important resources for quantum information [1–3]. It plays a central role in many applications, i.e., quantum precision measurements [4], fault tolerant quantum computation [5,6], quantum networks [7–9], and many meaningful quantum technologies. Quantum teleportation [10,11], as a celebrated quantum technology involving entanglement, aims to artfully transfer the quantum state between the different physical carriers. Here we consider a different scenario where the polarization degree of freedom (DoF) on Alice's side is convenient for quantum information processing, but the orbital angular momentum (OAM) DoF on Bob's side is advanced. A quantum task is thus raised to transmit a polarization encoding state from Alice to an OAM encoding qubit on Bob's side. This quantum task can be solved by virtue of a teleportation-based method.

Quantum teleportation is a fundamental protocol in quantum information with no classical analog [10,11]. It allows for the simulation of an ideal quantum channel by exploiting entanglement and classical communication. One of the most important features of quantum teleportation is that a quantum state can be transmitted faithfully, even though the state itself is completely unknown to the sender and the receiver as well. In past decades, quantum teleportation has been extensively developed on many physical platforms, such as linear optics [12,13], trapped ions [14–16], superconducting circuits [17,18], even some high-dimensional systems [19–21], hybrid-DoF discrete systems [22–24], and hybrid-entangled systems between continuous and discrete variables [25–29].

In addition, realizing a complete Bell-state measurement (BSM) is still a major issue for quantum teleportation, which directly affects the efficiency of the quantum state transfer. Recall that the simplest BSM scenario in linear optics with the necessary single-photon detectors only allows, at most, two of the four Bell states to be distinguished, and the corresponding Bell efficiency is constrained to be 50% [30,31]. To improve the Bell efficiency as much as possible, many schemes have been presented in past years. For example, Ref. [32] has employed the extra time DoF to achieve this mission and its Bell efficiency could be promoted into 100% in principle. Reference [33] has proposed an arbitrary bipartite high-dimensional BSM configuration with the auxiliary entanglement. Reference [34] has exploited the technologies of hyperentanglement, which divided the 16 hyperentangled Bell states into 14 groups. This theoretical possibility clearly implies an overhead of quantum resources that is a nontrivial experimental challenge. Solving this problem is an active area of research [32–34].

In this paper, our work mainly focuses on the quantum state transfer on the photon (also named "flying qubit") that is the most ideal transmission and processing carrier of information [35]. Particularly, the polarization DoF of the photon is frequently employed for coding a variety of information [12,36]. Apart from the polarization DoF, the photonic transverse spatial mode DoF [37–39] has attracted wide attention recently due to its broad prospects in the area of quantum communication. By way of illustration, Zeilinger *et al.* [40] has distributed the entangled photons directly through the atmosphere to a receiver station 7.8 km away over the city of Vienna, and they [41,42] have also verified quantum entanglement of photon pairs with spatial modes over a turbulent, real-world link of 3 km across Vienna. Forbes *et al.* has demonstrated the feasibility of transferring the multidimensional OAM

*yunlong.wang@mail.xjtu.edu.cn

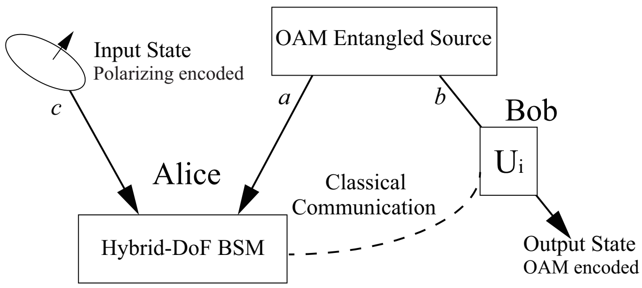

FIG. 1. Scheme of quantum state transfer. A polarization input state c at Alice is transmitted to Bob using a shared OAM maximum entangled state $|\phi_-\rangle_{ab}$ and a classical communication channel. Alice performs a hybrid-DoF Bell state measurement on her systems, a and c, and communicates the outcome to Bob. Bob can check his qubit b under the conditional outcome information from Alice.

entangled states over 250 m through the single-mode fiber [43]. Cao *et al.* has reported the three-dimensional OAM entanglement distribution via a 1-km-long fewer-mode optical fiber by using an actively stabilizing phase precompensation technique [44].

In this work, we implement the quantum state transfer of different photons from the polarization space to the OAM space. This paper is organized as follows. In Sec. II, the experimental proposal is introduced, which intriguingly combines the conventional teleportation protocol [45] with a presented hybrid-DoF BSM. Moreover, we show that the Bell efficiency of this hybrid-DoF BSM can be theoretically reached 100%. In Sec. III, the experimental setup and results are exhibited in detail. We use six states of poles of the Bloch sphere to test our scheme, with the fidelity of the quantum state transfer being $91.8 \pm 1.3\%$. Our work gives a reasonable polarization-OAM quantum interface solution for the quantum state transfer, and contributes a hybrid-entangled BSM approach for achieving a tangible Bell-efficiency enhancement. Section IV provides a conclusion and discussion.

II. EXPERIMENTAL PROPOSAL

Our experimental proposal is shown in Fig. 1. We consider two parties—Alice and Bob—who share two qubits of OAM DoF, a and b. The two qubits are prepared in a maximally OAM entangled state, which is generated by a Hong-Ou-Mandel (HOM) interference [46–48]. Let us consider two photons that are incident on two input ports of a beam splitter (BS), respectively. When arriving at input ports of the BS, the two photons are in the state

$$|\psi_{\rm in}\rangle_{ab} = \hat{a}_j^\dagger \hat{b}_k^\dagger |{\rm vacuum}\rangle_{ab} = |1; j\rangle_a |1; k\rangle_b, \quad (1)$$

where $\hat{a}_j^\dagger$ and $\hat{b}_k^\dagger$ are creation operators of photons in the a and b modes of BS, respectively. The subscripts j and k denote other properties of the photons, which determine how distinguishable they are, such as polarization and transverse spatial modes, and so on. Specifically, we consider that two photons interfere on a 50:50 BS. If the two photons are in different polarization states, i.e., one is in $|H\rangle$ and another in $|V\rangle$, the corresponding output state is

$$|\psi_{\rm out}\rangle_{ab} = \tfrac{1}{2}(|2; H, V\rangle_a + |2; H, V\rangle_b + |1; H\rangle_a |1; V\rangle_b - |1; V\rangle_a |1; H\rangle_b). \quad (2)$$

The first and second terms of the state represent the case where the two photons simultaneously exit out of the same port of the BS (photon bunching), and the last two components describe the situation where the two photons leave out of different ports (photon antibunching), respectively. If the two photons are in the same polarization state, i.e., $|H\rangle_a |H\rangle_b$, the corresponding output state is

$$|\psi_{\rm out}\rangle_{ab} = \frac{1}{\sqrt{2}}(|2; H, H\rangle_a - |2; H, H\rangle_b). \quad (3)$$

The OAM maximally entangled state, $|\phi_-\rangle_{ab} = (|+\ell_0\rangle_a |+\ell_0\rangle_b - |-\ell_0\rangle_a |-\ell_0\rangle_b)/\sqrt{2}$ (known as a Bell pair), can be generated in a similar way. For convenience, $|\pm\ell_0\rangle$ denote OAM states with different OAM values of $\ell = +1$ and $\ell = -1$, respectively. When a pair of input photons is in the same OAM state ($|+\ell_0\rangle$), since its spatial mode will be flipped after reflection, the output state is

$$|\psi_{\rm out}\rangle_{ab} = \tfrac{1}{2}(|2; +\ell_0, -\ell_0\rangle_a + |2; +\ell_0, -\ell_0\rangle_b + |1; +\ell_0\rangle_a |1; +\ell_0\rangle_b - |1; -\ell_0\rangle_a |1; -\ell_0\rangle_b). \quad (4)$$

Since the present experimental scheme has a postselection count coincidence between modes a and b, and the first and second components of (4) are automatically filtered, the state (4) is just the entangled state $|\phi_-\rangle_{ab}$ required for our experimental scheme.

As shown in Fig. 1, Alice and Bob share the entangled state $|\phi_-\rangle_{ab}$; meanwhile, another qubit c in the polarizing state $|\psi\rangle_c$ is sent to Alice,

$$|\psi\rangle_c = \alpha|H\rangle_c + \beta|V\rangle_c, \quad (5)$$

where $\alpha^2 + \beta^2 = 1$ and Bob does not know any information of the state. The whole hybrid-DoF quantum state which Alice and Bob hold can be written as

$$\begin{aligned}|\Psi\rangle &= |\psi\rangle_c \otimes |\phi_-\rangle_{ab} \\ &= (\alpha|H\rangle_c + \beta|V\rangle_c) \\ &\otimes \frac{1}{\sqrt{2}}(|+\ell_0\rangle_a |+\ell_0\rangle_b - |-\ell_0\rangle_a |-\ell_0\rangle_b). \end{aligned} \quad (6)$$

We define the four hybrid-entangled Bell states in OAM and polarization DoFs,

$$\begin{aligned}|\omega_{ca}^\pm\rangle &= \frac{1}{\sqrt{2}}(|H\rangle_c |+\ell_0\rangle_a \pm |V\rangle_c |-\ell_0\rangle_a), \\ |\xi_{ca}^\pm\rangle &= \frac{1}{\sqrt{2}}(|H\rangle_c |-\ell_0\rangle_a \pm |V\rangle_c |+\ell_0\rangle_a). \end{aligned} \quad (7)$$

In terms of these states, Eq. (6) can be rewritten as

$$\begin{aligned}|\Psi\rangle = \tfrac{1}{2}[&|\omega_{ca}^+\rangle(\alpha|+\ell_0\rangle_b - \beta|-\ell_0\rangle_b) \\ &+ |\omega_{ca}^-\rangle(\alpha|+\ell_0\rangle_b + \beta|-\ell_0\rangle_b) \\ &+ |\xi_{ca}^+\rangle(\beta|+\ell_0\rangle_b - \alpha|-\ell_0\rangle_b) \\ &- |\xi_{ca}^-\rangle(\beta|+\ell_0\rangle_b + \alpha|-\ell_0\rangle_b)]. \end{aligned} \quad (8)$$

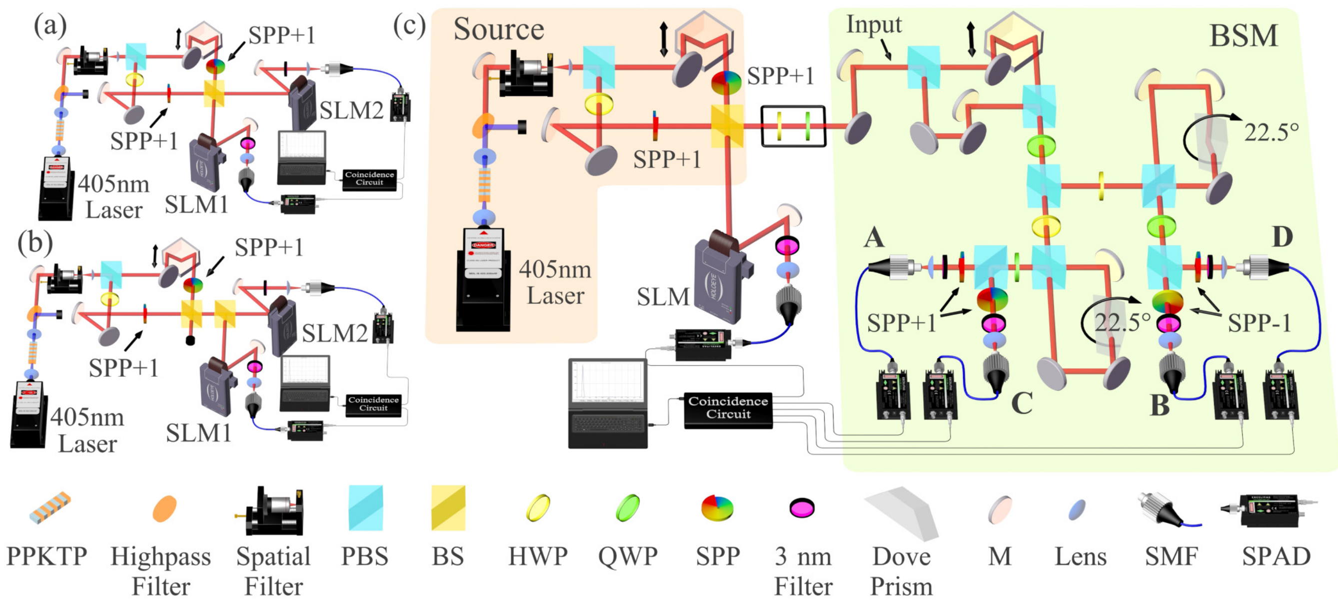

FIG. 2. Experimental setup, (a),(b) Measurement of OAM quantum states in antibunching and bunching, respectively. (c) Experimental setup for polarization-OAM quantum state transfer, in which the OAM entangled source is located in the pink box, any polarization quantum state of Alice's qubit c can be prepared by the HWP and QWP located in the black box (Between Source and BSM Parts), and the hybrid-DoFs (OAM and polarization) Bell-state measurement is located in the green box. PPKTP: poled potassium titanyl phosphate; PBS: polarizing beam splitter; BS: beam splitter; HWP: half-wave plate; QWP: quarter-wave plate; SPP: spiral phase plate; M: mirror; SMF: single-mode fiber; SPAD: single-photon avalanche detector.

A vital step for our experimental scheme is to perform a perfect BSM of qubits c and a, projecting them onto the basis of the four hybrid-entangled Bell states (7), and discriminating each one of them. In our scenario, Alice performs a complete BSM, which projects her qubits a and c into one of the four Bell states. As a result, the state of the input qubit collapses due to the measurement; meanwhile, the qubit b in Bob's side is simultaneously projected onto the certain quantum state that is different from the input state only by a unitary transformation. In the feed-forward step, Alice communicates the outcome of her measurement through a classical channel with Bob, who then applies the corresponding unitary operation to recover the original input state on the qubit b. Similarly, for experimental verification, Bob only needs to distinguish quantum state on qubit c after classical communication and observe whether it is consistent.

Note that Alice's input state is assumed to be unknown; otherwise it reduces to remote state preparation. In typical experiments, the input state is taken to be pure and belonging to a limited alphabet, for example, the six poles of the Bloch sphere. In the presence of decoherence, the quality of the reconstructed state may be quantified by its fidelity $F \in (0, 1]$. This is the fidelity between Alice's input state and Bob's output state, averaged over all the outcomes of the BSM and input state alphabet. In the original teleportation scheme, for small values of the fidelity, strategies exist that allow for an imperfect teleportation while making no use of any entangled resource. For example, Alice may directly measure her input state, thereby sending the results to Bob for him to prepare an output state. Such a measure-prepare strategy is known as "classical teleportation" and has the maximum fidelity $F_{\text{class}} = 2/3$ for an arbitrary input state or, equivalently, an alphabet of mutually unbiased states, such as the six poles of the Bloch sphere. Thus, the requirement $F > F_{\text{class}}$ is a clear benchmark for ensuring that quantum resources are utilized [49].

III. EXPERIMENTAL SETUP AND RESULTS

Figure 2 shows the experimental setup for polarization-OAM quantum state transfer. A continuous wave laser with center wavelength at 405 nm is used to pump a 2-mm-long linear crystal of periodically poled potassium titanyl phosphate (PPKTP), cutting for degenerate type-II collinear phase

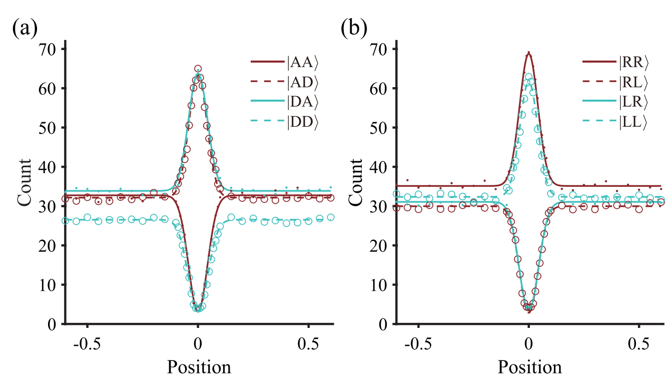

FIG. 3. Two-photon OAM HOM interference results for Fig. 2(a) on different measurement bases, where $|D\rangle = (|+\ell_0\rangle + |-\ell_0\rangle)/\sqrt{2}$, $|A\rangle = (|+\ell_0\rangle - |-\ell_0\rangle)/\sqrt{2}$, $|R\rangle = (|+\ell_0\rangle + \mathrm{i}|-\ell_0\rangle)/\sqrt{2}$, and $|L\rangle = (|+\ell_0\rangle - \mathrm{i}|-\ell_0\rangle)/\sqrt{2}$. Since the fitting curves are close to each other and the error bars are small under the coordinate of this figure, error bars are not drawn, for a better presentation.

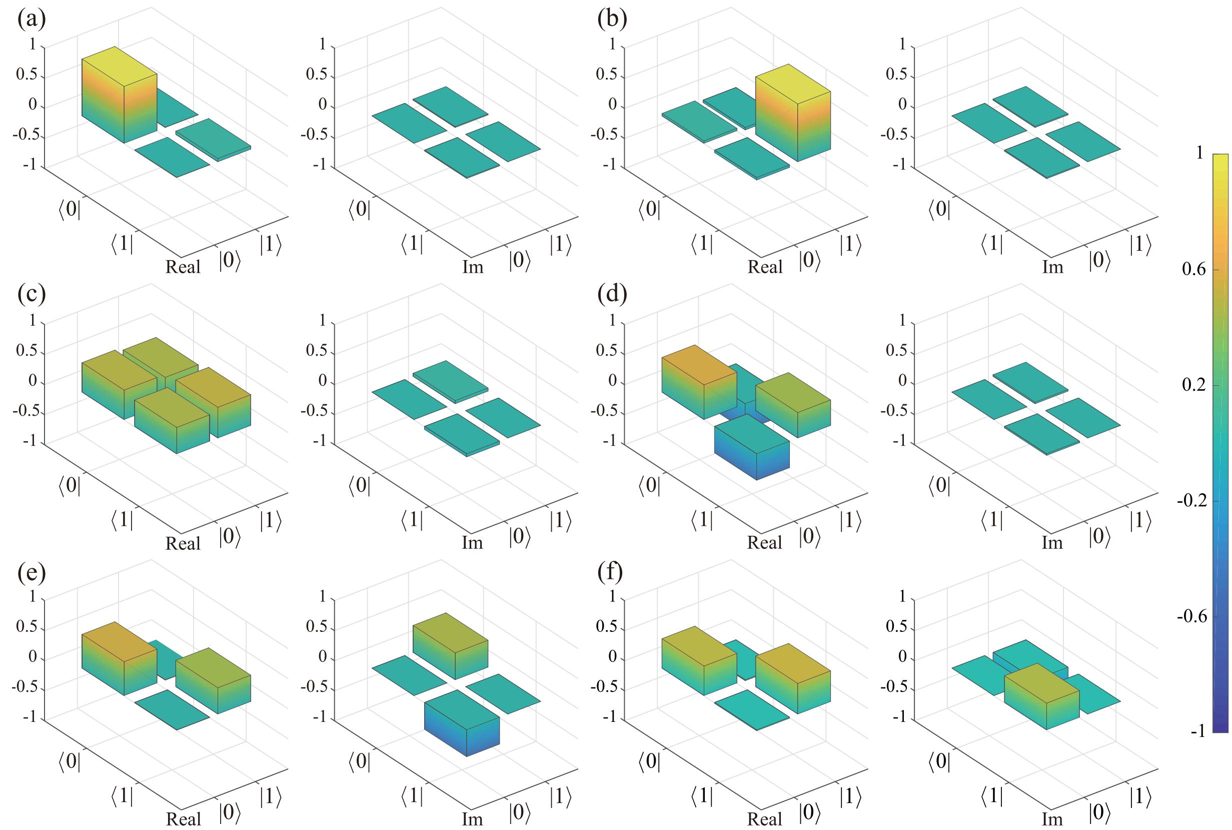

FIG. 4. Tomography of the transmitted states. The input states prepared on qubit c are the six poles of the Bloch sphere, $|0\rangle = |H\rangle$, $|1\rangle = |V\rangle$, $|D\rangle = (|H\rangle + |V\rangle)/\sqrt{2}$, $|A\rangle = (|H\rangle - |V\rangle)/\sqrt{2}$, $|R\rangle = (|H\rangle + \mathrm{i}|V\rangle)/\sqrt{2}$, and $|L\rangle = (|H\rangle - \mathrm{i}|V\rangle)/\sqrt{2}$, respectively. Colored bars show the experimental results.

matching which emits correlated photon pairs at 810 nm. Photons from the source are spatially filtered to the fundamental Gaussian mode using a spatial filter. The polarizing beam splitter (PBS) is used to separate correlated photon pairs. A half-wave plate (HWP) is used to make the polarizations of correlated photon pairs consistent, and spiral phase plates (SPP, topological charge +1) are used to modulate photon pairs in the same OAM state, $|+\ell_0\rangle$.

There is a motorized translation stage in the Mach-Zehnder interferometer, which is used to control the time difference of correlated photon pairs to the BS. Its traveling range is 27 mm, and the minimum incremental motion is 0.2 μm. As shown by formula (4), due to the OAM HOM interference of photon pairs at the BS, both the antibunching and bunching components exist. Experimentally, we use the setups illustrated in Figs. 2(a) and 2(b) to study the aforementioned two-photon correlation characteristics, respectively. For detection, a spatial light modulator (SLM) together with a SMF is used to perform any directional projection measurements of the OAM modes. The coincidence counts of two single-photon avalanche detectors are proportional to the detected correlated photon pairs.

We have measured eight kinds of two-photon joint measurements for Fig. 2, and its results are shown in Fig. 3, in which the position from -0.6 to 0.6 mm is the range of movement of the motorized translation stage. It can be observed that the half width of HOM interference is about 194 μm as the narrowband of filters used here is 3 nm. Therefore, the OAM entangled state $|\phi_-\rangle_{ab}$, i.e., antibunching part in Eq. (4), is generated at the origin of the coordinate. The fidelity between the theoretical state $|\phi_-\rangle_{ab}$ and experimentally prepared state is $92.55 \pm 1.02\%$. Similarly for Fig. 2(b), we have checked the bunching part in Eq. (4) and its fidelity is $93.13 \pm 1.21\%$.

The transmitted qubit here is encoded in polarization DoF and can be prepared in an arbitrary pure state by the HWP and QWP, which are located in the black box. Now let us turn to BSM, which is a vital step for our experiment. For multi-DoF systems, a complete BSM can be realized without any auxiliary qubits. As shown in the green part of Fig. 2(c), we can experimentally realize a complete polarization-OAM hybrid-entangled BSM in a single photon, whereby all of the four Bell states, $|\omega_{ca}^{\pm}\rangle$ and $|\xi_{ca}^{\pm}\rangle$, are finally transmitted to four different ports, respectively. This BSM scheme can be described by four steps, as follows:

(1) The Mach-Zehnder interferometer and the QWP at 45° (both head and tail are PBSs, and only one reflection difference between the two paths) make all four Bell states ($|\omega_{ca}^{\pm}\rangle$ and $|\xi_{ca}^{\pm}\rangle$) change from nonseparate states to separate states ($|H\rangle|+\ell_0\rangle$, $|V\rangle|-\ell_0\rangle$, $|H\rangle|-\ell_0\rangle$, and $|V\rangle|+\ell_0\rangle$).

(2) Two of the four separate states are then projected through the PBS and another two are reflected due to their polarizations.

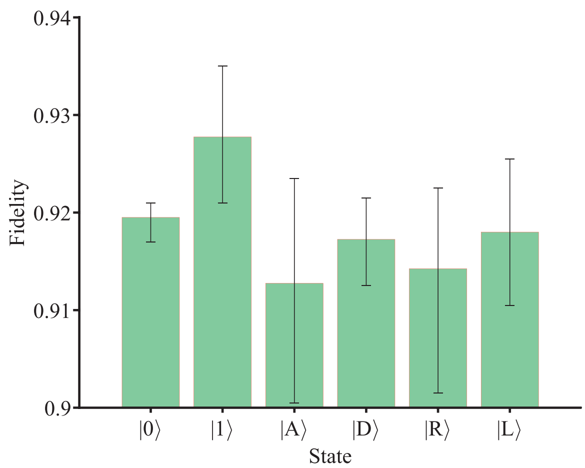

FIG. 5. Fidelities of teleported states. The fidelity is calculated according to $F = \langle\psi|\rho|\psi\rangle$, where $|\psi\rangle$ is one of the six mutually unbiased basis states. All fidelities are greater than the classical teleportation bound, $F_{\text{class}} = 2/3$.

(3) The HWP, Sagnac interferometer, QWP, and final PBS are made up of a OAM ±1 sorter [50].

(4) Finally, SPPs ($+1$ or -1 in Fig. 2) here are also to flatten the photons' phase into a Gaussian mode that can be efficiently coupled into the SMF.

As mentioned above, all four Bell states can be discriminated in our experimental scheme, and there is no probabilistic photon loss in theory.

In Sec. II, we have discussed that an alphabet of mutually unbiased states, such as the six poles of the Bloch sphere, can be used to test the present scheme based on quantum teleportation. We only need to check whether the fidelities for these input states are greater than F_{class} to ensure the use of quantum resources. Figure 4 shows the teleported states' tomography, which are reconstructed using a maximum likelihood estimator of the density matrix. Figure 5 shows the fidelities for each of the six input states. It can be seen that the six input states are well reproduced, and all these fidelities are greater than F_{class}, indicating that it is actually a nonclassical cloning experiment. In addition, for all the data in the above measurements, we also have counted the ratio of coincidence events of the four ports A, B, C, and D (see Fig. 2). The results are listed in Table I, which is consistent with the theoretical probabilities (all being 0.25) for four Bell states.

TABLE I. Ratio of counting probabilities of four ports (which have been normalized).

Captures	A	B	C	D
Theory (%)	25	25	25	25
Experiment (%)	23.8 ± 1.3	25.4 ± 1.2	24.6 ± 0.8	26.2 ± 1.1

IV. CONCLUSION AND DISCUSSION

In summary, we have experimentally demonstrated a process of quantum state transfer from one photon's polarization DoF to another photon's OAM DoF with a $91.8 \pm 1.3\%$ average fidelity. We remind the reader that although our transmitted state is known by Alice, this scheme has some similar advantages to original teleportation. One is that the transfer of the materials' bodies is not required. Another one is that only a part of the information of the state is transferred via a classical channel. In other words, the state is protected from Eve. In some sense, it could also be recognized as a kind of interface for the quantum state transfer between the different particles and different DoFs. This interface offers a probability that makes it employable in other hybrid quantum systems. Meanwhile, we have verified experimentally that the hybrid-DoF BSM proposed in this paper can indeed achieve a higher Bell efficiency since all of the four hybrid-entangled Bell states can be discriminated well. In addition, as far as the usage of the OAM DoF, one motivation is mainly inspired by its high-dimensional characteristic for quantum information processing ($\ell = \pm1, \pm2, \dots$). Although ℓ is limited to ±1 values in this experiment, the value of ℓ can actually be set into any integers for each state by changing the SPP in the entanglement source and in the BSM projection, in principle. Furthermore, our polarization-orbital coupled BSM scheme is entitled to be employed for OAM to polarization quantum state transfer and dense coding.

ACKNOWLEDGMENTS

This work was supported in part by the National Nature Science Foundation of China (Grants No. 11534008, No. 11804271, No. 91736104, and No. 12074307), Ministry of Science and Technology of China (Grant No. 2016YFA0301404), and China Postdoctoral Science Foundation via Project No. 2020M673366.

[1] M. A. Nielsen and I. L. Chuang, *Quantum Computation and Quantum Information* (Cambridge University Press, New York, 2010).

[2] R. Horodecki, P. Horodecki, M. Horodecki, and K. Horodecki, Quantum entanglement, Rev. Mod. Phys. **81**, 865 (2009).

[3] M. Erhard, M. Krenn, and A. Zeilinger, Advances in high-dimensional quantum entanglement, Nat. Rev. Phys. **2**, 365 (2020).

[4] V. Giovannetti, S. Lloyd, and L. Maccone, Advances in quantum metrology, Nat. Photon. **5**, 222 (2011).

[5] D. Gottesman, Theory of fault-tolerant quantum computation, Phys. Rev. A **57**, 127 (1998).

[6] S. Omkar, Y. S. Teo, and H. Jeong, Resource-Efficient Topological Fault-Tolerant Quantum Computation with Hybrid Entanglement of Light, Phys. Rev. Lett. **125**, 060501 (2020).

[7] H. J. Kimble, The quantum internet, Nature (London) **453**, 1023 (2008).

[8] C. Simon, Towards a global quantum network, Nat. Photon. **11**, 678 (2017).

[9] S. Wehner, D. Elkouss, and R. Hanson, Quantum internet: A vision for the road ahead, Science **362**, aam9288 (2018).

[10] S. Pirandola, J. Eisert, C. Weedbrook, A. Furusawa, and S. L. Braunstein, Advances in quantum teleportation, Nat. Photon. **9**, 641 (2015).
[11] A. Zeilinger, Quantum teleportation, onwards and upwards, Nat. Phys. **14**, 3 (2018).
[12] D. Bouwmeester, J.-W. Pan, K. Mattle, M. Eibl, H. Weinfurter, and A. Zeilinger, Experimental quantum teleportation, Nature (London) **390**, 575 (1997).
[13] X.-L. Wang, X.-D. Cai, Z.-E. Su, M.-C. Chen, D. Wu, L. Li, N.-L. Liu, C.-Y. Lu, and J.-W. Pan, Quantum teleportation of multiple degrees of freedom of a single photon, Nature (London) **518**, 516 (2015).
[14] M. D. Barrett, J. Chiaverini, T. Schaetz, J. Britton, W. M. Itano, J. D. Jost, E. Knill, C. Langer, D. Leibfried, R. Ozeri, and D. J. Wineland, Deterministic quantum teleportation of atomic qubits, Nature (London) **429**, 737 (2004).
[15] M. Riebe, H. Häffner, C. F. Roos, W. Hänsel, J. Benhelm, G. P. T. Lancaster, T. W. Körber, C. Becher, F. Schmidt-Kaler, D. F. V. James, and R. Blatt, Deterministic quantum teleportation with atoms, Nature (London) **429**, 734 (2004).
[16] C. Nölleke, A. Neuzner, A. Reiserer, C. Hahn, G. Rempe, and S. Ritter, Efficient Teleportation between Remote Single-Atom Quantum Memories, Phys. Rev. Lett. **110**, 140403 (2013).
[17] M. Baur, A. Fedorov, L. Steffen, S. Filipp, M. P. da Silva, and A. Wallraff, Benchmarking a Quantum Teleportation Protocol in Superconducting Circuits Using Tomography and an Entanglement Witness, Phys. Rev. Lett. **108**, 040502 (2012).
[18] L. Steffen, Y. Salathe, M. Oppliger, P. Kurpiers, M. Baur, C. Lang, C. Eichler, G. Puebla-Hellmann, A. Fedorov, and A. Wallraff, Deterministic quantum teleportation with feed-forward in a solid state system, Nature (London) **500**, 319 (2013).
[19] C. Zhang, J. F. Chen, C. Cui, J. P. Dowling, Z. Y. Ou, and T. Byrnes, Quantum teleportation of photonic qudits using linear optics, Phys. Rev. A **100**, 032330 (2019).
[20] Y.-H. Luo, H.-S. Zhong, M. Erhard, X.-L. Wang, L.-C. Peng, M. Krenn, X. Jiang, L. Li, N.-L. Liu, C.-Y. Lu, A. Zeilinger, and J.-W. Pan, Quantum Teleportation in High Dimensions, Phys. Rev. Lett. **123**, 070505 (2019).
[21] X.-M. Hu, C. Zhang, B.-H. Liu, Y. Cai, X.-J. Ye, Y. Guo, W.-B. Xing, C.-X. Huang, Y.-F. Huang, C.-F. Li, and G.-C. Guo, Experimental High-Dimensional Quantum Teleportation, Phys. Rev. Lett. **125**, 230501 (2020).
[22] S.-W. Lee and H. Jeong, Near-deterministic quantum teleportation and resource-efficient quantum computation using linear optics and hybrid qubits, Phys. Rev. A **87**, 022326 (2013).
[23] A. Z. Khoury and P. Milman, Quantum teleportation in the spin-orbit variables of photon pairs, Phys. Rev. A **83**, 060301(R) (2011).
[24] L. Chen and W. She, Teleportation of a controllable orbital angular momentum generator, Phys. Rev. A **80**, 063831 (2009).
[25] D. V. Sychev, A. E. Ulanov, E. S. Tiunov, A. A. Pushkina, A. Kuzhamuratov, V. Novikov, and A. Lvovsky, Entanglement and teleportation between polarization and wave-like encodings of an optical qubit, Nat. Commun. **9**, 3672 (2018).
[26] A. E. Ulanov, D. Sychev, A. A. Pushkina, I. A. Fedorov, and A. I. Lvovsky, Quantum Teleportation between Discrete and Continuous Encodings of an Optical Qubit, Phys. Rev. Lett. **118**, 160501 (2017).
[27] S. Takeda, T. Mizuta, M. Fuwa, P. Van Loock, and A. Furusawa, Deterministic quantum teleportation of photonic quantum bits by a hybrid technique, Nature (London) **500**, 315 (2013).
[28] S. Takeda, M. Okada, and A. Furusawa, Optical hybrid quantum teleportation and its applications, in *Quantum Communications and Quantum Imaging XV, Vol. 10409*, edited by R. E. Meyers, Y. Shih, and K. S. Deacon, International Society for Optics and Photonics (SPIE, 2017), pp. 31–41.
[29] M. Huo, J. Qin, J. Cheng, Z. Yan, Z. Qin, X. Su, X. Jia, C. Xie, and K. Peng, Deterministic quantum teleportation through fiber channels, Sci. Adv. **4**, eaas9401 (2018).
[30] N. Lütkenhaus, J. Calsamiglia, and K. A. Suominen, Bell measurements for teleportation, Phys. Rev. A **59**, 3295 (1999).
[31] L. Vaidman and N. Yoran, Methods for reliable teleportation, Phys. Rev. A **59**, 116 (1999).
[32] B. P. Williams, R. J. Sadlier, and T. S. Humble, Superdense Coding Over Optical Fiber Links with Complete Bell-State Measurements, Phys. Rev. Lett. **118**, 050501 (2017).
[33] H. Zhang, C. Zhang, X.-M. Hu, B.-H. Liu, Y.-F. Huang, C.-F. Li, and G.-C. Guo, Arbitrary two-particle high-dimensional bell-state measurement by auxiliary entanglement, Phys. Rev. A **99**, 052301 (2019).
[34] C.-Y. Gao, B.-C. Ren, Y.-X. Zhang, Q. Ai, and F.-G. Deng, Universal linear-optical hyperentangled bell-state measurement, Appl. Phys. Express **13**, 027004 (2020).
[35] A. K. Ekert, Quantum Cryptography Based on Bell's Theorem, Phys. Rev. Lett. **67**, 661 (1991).
[36] K. Mattle, H. Weinfurter, P. G. Kwiat, and A. Zeilinger, Dense Coding in Experimental Quantum Communication, Phys. Rev. Lett. **76**, 4656 (1996).
[37] M. Erhard, R. Fickler, M. Krenn, and A. Zeilinger, Twisted photons: New quantum perspectives in high dimensions, Light: Sci. Appl. **7**, 17146 (2018).
[38] A. Forbes and I. Nape, Quantum mechanics with patterns of light: Progress in high dimensional and multidimensional entanglement with structured light, AVS Quantum Sci. **1**, 011701 (2019).
[39] J. Wang, F. Castellucci, and S. Franke-Arnold, Vectorial light–matter interaction: Exploring spatially structured complex light fields, AVS Quantum Sci. **2**, 031702 (2020).
[40] K. Resch, M. Lindenthal, B. Blauensteiner, H. Böhm, A. Fedrizzi, C. Kurtsiefer, A. Poppe, T. Schmitt-Manderbach, M. Taraba, R. Ursin, P. Walther, H. Weier, H. Weinfurter, and A. Zeilinger, Distributing entanglement and single photons through an intra-city, free-space quantum channel, Opt. Express **13**, 202 (2005).
[41] M. Krenn, J. Handsteiner, M. Fink, R. Fickler, and A. Zeilinger, Twisted photon entanglement through turbulent air across vienna, Proc. Natl. Acad. Sci. **112**, 14197 (2015).
[42] M. Krenn, R. Fickler, M. Fink, J. Handsteiner, M. Malik, T. Scheidl, R. Ursin, and A. Zeilinger, Communication with spatially modulated light through turbulent air across Vienna, New J. Phys. **16**, 113028 (2014).
[43] J. Liu, I. Nape, Q. Wang, A. Vallés, J. Wang, and A. Forbes, Multidimensional entanglement transport through single-mode fiber, Sci. Adv. **6**, eaay0837 (2020).

[44] H. Cao, S.-C. Gao, C. Zhang, J. Wang, D.-Y. He, B.-H. Liu, Z.-W. Zhou, Y.-J. Chen, Z.-H. Li, S.-Y. Yu, J. Romero, Y.-F. Huang, C.-F. Li, and G.-C. Guo, Distribution of high-dimensional orbital angular momentum entanglement over a 1 km few-mode fiber, Optica **7**, 232 (2020).

[45] C. H. Bennett, G. Brassard, C. Crépeau, R. Jozsa, A. Peres, and W. K. Wootters, Teleporting an Unknown Quantum State via Dual Classical and Einstein-Podolsky-Rosen Channels, Phys. Rev. Lett. **70**, 1895 (1993).

[46] C. K. Hong, Z. Y. Ou, and L. Mandel, Measurement of Subpicosecond Time Intervals between Two Photons by Interference, Phys. Rev. Lett. **59**, 2044 (1987).

[47] Y. Yang, L. Xu, and V. Giovannetti, Exclusive Hong-Ou-Mandel zero-coincidence point, Phys. Rev. A **100**, 063810 (2019).

[48] F. Bouchard, A. Sit, Y. Zhang, R. Fickler, F. M. Miatto, Y. Yao, F. Sciarrino, and E. Karimi, Two photon interference: The Hong-Ou-Mandel effect, Rep. Prog. Phys. **84**, 012402 (2021).

[49] N. J. Cerf, N. Gisin, and S. Massar, Classical Teleportation of a Quantum Bit, Phys. Rev. Lett. **84**, 2521 (2000).

[50] D.-Z. Fu, J.-L. Jia, Y.-N. Zhou, D.-X. Chen, H. Gao, F.-L. Li, and P. Zhang, Realization of orbital angular momentum sorter of photons based on Sagnac interferometer, Acta Phys. Sin. **64**, 130704 (2015).